J Pharmacokinet Pharmacodyn (2014) 41:173–185
DOI 10.1007/s10928-014-9355-3

ORIGINAL PAPER

Physiologically based pharmacokinetic modelling of methotrexate and 6-mercaptopurine in adults and children. Part 2: 6-mercaptopurine and its interaction with methotrexate

Kayode Ogungbenro · Leon Aarons · The CRESim & Epi-CRESim Project Groups

Received: 15 November 2013 / Accepted: 6 March 2014 / Published online: 21 March 2014

Abstract 6-mercaptopurine (6-MP) is a purine antimetabolite and prodrug that undergoes extensive intracellular metabolism to produce thionucleotides, active metabolites which have cytotoxic and immunosuppressive properties. Combination therapies involving 6-MP and methotrexate have shown remarkable results in the cure of childhood acute lymphoblastic leukaemia (ALL) in the last 30 years. 6-MP undergoes very extensive intestinal and hepatic metabolism following oral dosing due to the activity of xanthine oxidase leading to very low and highly variable bioavailability and methotrexate has been demonstrated as an inhibitor of xanthine oxidase. Despite the success recorded in the use of 6-MP in ALL, there is still lack of effect and life threatening toxicity in some patients due to variability in the pharmacokinetics of 6-MP. Also, dose adjustment during treatment is still based on toxicity. The aim of the current work was to develop a mechanistic model that can be used to simulate trial outcomes and help to improve dose individualisation and dosage regimen optimisation. A physiological based pharmacokinetic model was proposed for 6-MP, this model has compartments for stomach, gut lumen, enterocyte, gut tissue, spleen, liver vascular, liver tissue, kidney vascular, kidney tissue, skin, bone marrow, thymus, muscle, rest of body and red blood cells. The model was based on the assumption of the same elimination pathways in adults and children. Parameters of the model include physiological parameters and drug-specific parameter which were obtained from the literature or estimated using plasma and red blood cell concentration data. Age-dependent changes in parameters were implemented for scaling and variability was also introduced on the parameters for prediction. Inhibition of 6-MP first-pass effect by methotrexate was implemented to predict observed clinical interaction between the two drugs. The model was developed successfully and plasma and red blood cell concentrations were adequately predicted both in terms of mean prediction and variability. The predicted interaction between 6-MP and methotrexate was slightly lower than the reported clinical interaction between the two drugs. The model can be used to predict plasma and tissue concentration in adults and children following oral and intravenous dosing and may ultimately help to improve treatment outcome in childhood ALL patients.

Keywords 6-mercaptopurine · Pharmacokinetics · PBPK · Leukaemia · Arthritis · Modelling

Abbreviation

6-MP	6-Mercaptopurine
MTX	Methotrexate
ALL	Acute lymphoblastic leukaemia
PK	Pharmacokinetics
PBPK	Physiologically based pharmacokinetic
RBC	Red blood cell
XO	Xanthine oxidase
HPRT	Hypoxanthine phosphoribosyltransferase
TPMT	Thiopurine methyltransferase
6-TGN	6-Thioguanine nucleotides
6-mMPN	6-Methylmercaptopurine nucleotide
BSA	Body surface area
BW	Body weight
HT	Height
AUC	Area under the concentration

The members of The CRESim & Epi-CRESim Project Groups is listed in Acknowledgment

K. Ogungbenro (✉) · L. Aarons
Centre for Applied Pharmacokinetic Research, Manchester Pharmacy School, The University of Manchester, Oxford Road, Manchester M13 9PT, UK
e-mail: kayode.ogungbenro@manchester.ac.uk

Introduction

6-mercaptopurine (6-MP) is a purine antimetabolite and a prodrug that undergoes extensive intracellular metabolism to produce thionucleotides the active metabolites [1]. 6-MP can be given both orally and intravenously and is widely used in the treatment of acute lymphoblastic leukaemia (ALL) and inflammatory bowel diseases [2, 3]. In the 1980s the use of combination chemotherapy involving methotrexate (MTX) and 6-MP in the treatment of childhood ALL emerged, this has led to remarkable improvement in cure (long term event free survival) from less than 10 % to more than 80 % today [4]. In most protocols, 6-MP is considered a very important and standard agent especially in maintaining remission.

6-MP undergoes very extensive intestinal and hepatic metabolism following oral dosing which has been linked to the activity of the xanthine oxidase (XO) enzyme in the gut and the liver leading to high first-pass metabolism. Consequently the bioavailability of orally administered 6-MP is very low and highly variable [5]. Although 6-MP can be given intravenously it is impracticable for use in maintenance treatment protocols especially in children and treatment of indications such as ALL which involves daily dosing for several years. The absorption of orally administered 6-MP is very rapid, with maximum concentrations reached within 1–2 h of dosing and the half-life is around 2 h [6]. The biotransformation of 6-MP is via three competing routes; XO, hypoxanthine phosphoribosyltransferase (HPRT) and thiopurine methyltransferase (TPMT) [7].

Despite the reported high variability in the PK of orally administered 6-MP and the complex relationship between 6-MP and its metabolites, therapeutic drug monitoring is still not routinely used for dose individualization and optimisation [8]. Modelling and simulation has been suggested as a useful tool for understanding variabilities, individualise doses and optimise dosage regimens in PK [9]. There have been very few attempts in the past towards developing a PK model for 6-MP. A PBPK was developed to simulate tissue concentration of 6-MP in rats, and also scaled to human, this model has compartments for plasma, kidney, liver, muscle, spleen, bone marrow and gut lumen [10]. Other key tissues/organs were missing from the model and there was no mass balance in the system. Also the model implemented a three compartment model for the biliary secretion and enterohepatic recirculation of the drug in rat and human when there is no evidence for this. A population PK model was also published for 6-MP which describes the plasma concentration of 6-MP in plasma and intracellular RBC concentration of two metabolites; 6-thioguanine nucleotides and 6-methylmercaptopurine nucleotide [11]. The model also incorporates a dichotomous covariate model that describes the effect of TPMT mutation on the PK of 6-MP. This model was based on limited data and has not been widely tested. Also the model is an empirical model that cannot be extrapolated or scaled to different age groups and cannot be used to predict concentration in tissues.

In the treatment of ALL, the combination of 6-MP and MTX remains a very important cornerstone however biochemical, PK and pharmacodynamic (PD) interactions have been reported between the two drugs [12, 13]. A number of experimental and clinical studies have described the clinical outcome from the combination of 6-MP and MTX as synergistic [13]. In terms of PK, MTX has been described as an inhibitor of XO thereby increasing the bioavailability of orally administered 6-MP especially when high doses of MTX are given intravenously [1, 8, 13, 14].

The aim of the current work was to develop a PBPK model for 6-MP in childhood ALL. The proposed model incorporated PK interaction between 6-MP and MTX based on the effect of MTX on XO in the gut and the liver. The model will be used to simulate tissue concentrations in organs/tissues such as the RBC, bone marrow and thymus. The model will complement the PBPK model developed for MTX [15] in the CRESim (Child-Rare-Euro-Simulation) project which is an European Union funded project designed to evaluate the role of modelling and simulation in the development of drugs for rare diseases. In this sub-project the disease is childhood ALL and the drugs that have been selected for the treatment are MTX and 6-MP. The PBPK models developed for MTX and 6-MP will be combined with disease models developed under other work packages to obtain a PBPK-PD model for clinical trial simulation.

Methodology

PBPK model development and assumptions

The PBPK model proposed for 6-MP is made up of 15 compartments for the following organs/tissues: stomach, gut lumen, enterocyte, gut tissue, spleen, liver vascular, liver tissue, kidney vascular, kidney tissue, skin, bone marrow, thymus, muscle, rest of body and RBC. These compartments are displayed in Fig. 1. The compartments in this model are the same as the compartments in the model developed for MTX (Part 1 of this work). All the tissues/organs in this model were modelled using standard flow limited equation for PBPK model, given by

$$V_T \frac{dC}{dt} = Q_T \left(C_P - \frac{C_T}{K_{p,T}} \right) \quad (1)$$

where V_T, C_T, Q_T and $K_{p,T}$ are the volume of distribution, concentration, plasma flow and tissue/plasma concentration

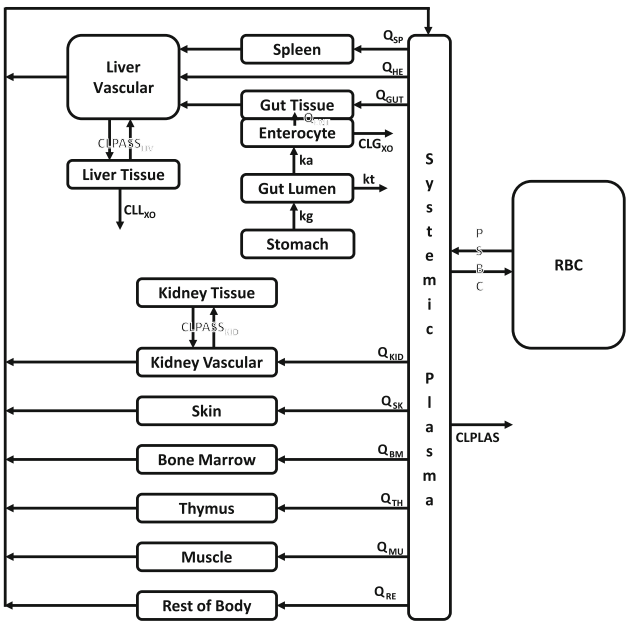

Fig. 1 Physiologically based pharmacokinetic model for 6-MP

ratio for the tissues and C_P is the systemic plasma concentration.

The liver and kidney were separated into vascular and tissue compartments with passive clearances between the two compartments and this was set to 10,000 times the value of plasma flows to these organs. This allows a flow limited assumption to be preserved in the organs. The volumes of the vascular compartments were set to 10 % of the volumes of the organs. Intracellular RBC 6-MP concentration was modelled assuming the drug exchange between the cells and plasma was characterised by the permeability-surface area product, *PSBC* assuming passive diffusion. Intracellular binding was assumed to be an instantaneous reaction, characterised by the number of binding sites, *nP* and dissociation constant, K_D [16, 17]. One or more of the enzymes responsible for the metabolism of 6-MP are present in each of the organs/tissues of the PBPK and as there is limited information in the literature on the activities of these enzymes in the tissues, it will be almost impossible to account for the activity of these enzymes explicitly in each of the organs/tissues. Based on in vivo 6-MP plasma concentration data obtained from the literature [5, 18], it is possible to separate XO activity in the gut and liver, the other routes of elimination were combined into a single parameter. A first order process was assumed for the absorption of 6-MP from the gut lumen and complete absorption was assumed i.e. fraction absorbed, F_a is 1. The PK interaction between 6-MP and MTX was based on the assumption that MTX inhibits XO in the gut and in the liver.

System parameters

System parameters for adults, assumed to be 18–20 years old and 70 kg weight were obtained from the literature. These include organ/tissue volumes and plasma flows, intestinal transit and gastric empting rate constants. Other parameters include body surface area (BSA), height (HT), body weight (BW) and haematocrit. The values for these parameters in adults are shown in Tables 1 and 2. For scaling of the PBPK model, age-dependent changes in anatomical and physiological parameters such plasma flows, organs/tissue volumes and body size descriptors were obtained from the literature. Cardiac output was predicted for children using the equation described in Johnson et al. [19]. Reference values for BW and HT were obtained from the literature and these were used to predict BSA using the Haycock and Dubois equations [20, 21]. Reference values were obtained for different organ/tissue volumes and plasma flows at 0, 1, 5, 10 and 15 years old [22]. The reference values for plasma flows and organ/tissue volumes for children and adult were expressed as the fractions of the cardiac outputs and BW for the different ages respectively. Simple linear interpolation between fractions of plasma flows and organ/tissue volumes for the reference age groups was used to simulate for values in between the age groups, allowing simulation of values for plasma flows and organ/tissue volumes for any age between 0 and 18–20 years old. Reference values for BW, HT and haematocrit for children were also obtained from the literature and simple linear interpolation was also used to obtain values between reference age groups [22, 23].

Drug specific parameters and parameter estimation

Tissue/plasma concentration ratios (K_p) were predicted for each tissue using the equations proposed by Poulin and Theil [24], K_p for the rest of body was optimised so that the predicted volume of distribution at steady state (V_{SS}) is the same as the observed in vivo value using the following equation [25]

$$K_{p,REST} = \frac{V_{SS,Obs} - V_P - \sum K_{p,T} \cdot V_T}{70 - \sum V_T} \quad (2)$$

The same K_p was assumed for adults and children and values for different tissues are presented in Table 1. Fraction unbound in plasma was obtained from the literature [26, 27] and the same value was assumed for adults and children because it is not clear in the literature which plasma protein 6-MP binds to. The PBPK model in Fig. 1, described by differential equations in Appendix 1, was fitted to plasma and RBC concentration data obtained from the literature to obtain estimates for some parameters. Zimm et al. [5, 18] investigated the effect of inhibition of

Table 1 Organ/tissue volumes (V) and plasma flows (Q) for adults and tissue/plasma concentration ratio (K_p) for each tissue/organ in the PBPK model

Parameters	Organs/tissues										
	Plasma	Muscle	Kidney	Liver	Gut	Enterocyte	Skin	Bone marrow	Spleen	Thymus	Rest of body
V (L)[a]	2.9	29	0.3	1.8	1.7	0.1	3.3	1.2	0.15	0.025	–[b]
Q (L/h)[a]	196[c]	36.5	43.7	14	30	11.8	10.7	5.9	6.4	2.9	–[d]
K_p	–	0.8	0.83	0.82	0.85	–	0.78	0.64	0.84	0.84	0.2

[a] Obtained from references [22] and [34]

[b] $70 - \Sigma V_T$

[c] cardiac output

[d] $196 - \Sigma Q_T$

Table 2 Other system parameters used in the PBPK model for adults

Parameter	Definition	Value	Source
kg (h^{-1})	Stomach emptying rate constant	2	[22]
kt (h^{-1})	Intestinal transit rate constant	0.25	[22]
Q_{ENT} (L/h)	Enterocytic plasma flow	11.76	[35, 36]
V_{ENT} (L)	Volume of enterocyte	0.12	[35]
BSA (m^2)	Body surface area	1.85	[22]
HT (m)	Height	1.76	[22]
BW (kg)	Body weight	70	[22]
V_{RBC} (L)	Volume of RBC	2.4	[22]
HCT	Haematocrit	0.45	[22]

first-pass metabolism of 6-MP in rhesus monkey and human by allopurinol, a potent inhibitor of XO. In the study 6-MP was given as an intravenous bolus and oral doses on two different occasions and the experiment was repeated for both routes with co-administration of allopurinol. The reported mean plasma concentration profiles in humans on the four occasions were used for parameter estimation. 75 mg/m^2 of 6-MP was administered on all occasions to ALL children (mean age = 13 years and range 3–18 years) who were in complete remission and were receiving maintenance chemotherapy. During co-medication with allopurinol, 100 mg of allopurinol was given three times daily for 2 days before 6-MP dosing. Lafolie et al. [28] reported individual plasma and RBC 6-MP concentrations in children with acute ALL or non-Hodgkin lymphoma receiving oral maintenance therapy. Mean plasma and RBC concentrations obtained from the reported individual concentrations were obtained and used for the parameter estimation. The children were 3–17 years old (mean age is 9.6 years) and the mean dose used was 59 mg/m^2. The data were used to estimate clearance parameters as well as RBC distribution parameters. The clearance parameters estimated were clearance due to XO in the gut (CLG_{XO}) and in the liver (CLL_{XO}) and clearance due to other enzymes ($CLPLAS$). RBC distribution parameters estimated were $PSBC$, nP and K_D. Because of the different ages of the children used in the data for estimation of clearance, parameters were normalised for a 70 kg adult using allometry and were also used for scaling to different age groups as follows [29]

$$CLG_{XO} = CLG_{XO,ad} \cdot \left(\frac{BW}{BW_{ad}}\right)^{0.75} \quad (3)$$

$$CLL_{XO} = CLL_{XO,ad} \cdot \left(\frac{BW}{BW_{ad}}\right)^{0.75} \quad (4)$$

$$CLPLAS = CLPLAS_{ad} \cdot \left(\frac{BW}{BW_{ad}}\right)^{0.75} \quad (5)$$

where $CLG_{XO,ad}$, $CLL_{XO,ad}$ and $CLPLAS_{ad}$ are the adult values for the clearance parameters and BW and BW_{ad} are the weight for an individual and adults respectively. RBC distribution parameters were assumed to be the same for adults and children but RBC volume changes with age.

Inhibition of 6-MP first-pass metabolism by MTX

Inhibition of the PK of 6-MP was modelled through inhibition of first-pass metabolism (inhibition of XO both in the gut and the liver). Competitive inhibition of the XO clearance parameters in the gut and the liver (CLG_{XO} and CLL_{XO}) was assumed and an inhibition constant reported in the literature was used [14, 30].

Variability

In order to simulate observed plasma concentrations in different age groups, variability was introduced on the system and drug-specific parameters. The main sources of variability in the PBPK model were via BW and BSA. Cardiac output was modelled as a function of BSA and through this variability was introduced to plasma flows for all the tissues/organs. Variability on BW was introduced into the model through organ/tissue volumes. Variability

was also introduced on other parameters such as *kg* (gastric emptying rate constant), *kt* (intestinal transit rate constant), CLG_{XO}, CLL_{XO}, *CLPLAS*, *PSBC*, *nP*, K_D and *ka* (absorption rate constant). A lognormal distribution for the distribution of the parameters and a CV of 20 % were assumed.

Simulations

To assess the performance of the proposed PBPK model, plasma concentration profiles were simulated for different age groups and compared with reported observed data. The model was assessed following both intravenous and oral dosing. Attempts were made to match simulations with the reported age and dose for the different studies. Mean doses for the studies were used for simulation and in most cases these were based on BSA. A virtual simulation of 1,000 subjects was performed in all cases and 2.5th, 50th and 97.5th percentiles were calculated and superimposed on the plot of observed data published in the literature. In some cases individual plasma or RBC concentration–time points were plotted and in others mean profiles with standard deviation (SD) or standard error bars (SE) for each time point were plotted. Data in graphs were digitized using GetData Graph Digitizer [31]. Simulations were also performed for the interaction using the models developed for MTX [15] and 6-MP and clinical studies were also matched in all cases in terms of dose and age.

Results

The $K_p s$ predicted for each tissue are shown in Table 2. Table 3 shows the other drug-specific parameters (clearance and RBC distribution parameters) used in the PBPK model, including the parameters that were estimated from fitting. The fitting was done in NONMEM v 7.2 [32]. All parameters were well estimated with a percentage standard error (*SE* %) less than 25 % except *nP* and K_D with *SE* % of 89 % and 39 % respectively. Figure 2 shows the plot of observed and predicted plasma and RBC concentrations for the fitting [18, 28]. Figure 2a shows the plasma concentration fitting for intravenous dosing of 6-MP with and without allopurinol; Fig. 2b shows the plasma concentration fitting for oral dosing of 6-MP with and without allopurinol; Fig. 2c shows the plasma concentration fitting for oral dosing of 6-MP without allopurinol; and Fig. 2d shows the RBC concentration fitting for oral dosing of 6-MP without allopurinol. Mean plasma and RBC concentrations were used in all cases and a satisfactory fitting of the PBPK model to the data was obtained.

Mean predicted plasma concentration profiles of 6-MP in plasma, muscle, kidney, liver, gut bone marrow, thymus and RBC were obtained for 5, 10 and 18 years individuals following oral dosing of 75/mg^2 is shown in Fig. 3. The profiles for the tissues except muscle are parallel to plasma profiles and this shows rapid distribution into these tissues. However for muscle it appears there is a delay in the distribution of the drug into the tissue. Comparing the three age groups, there is no significant difference between the profiles for 5 and 10 years old in terms of area under the concentration (AUC) and maximum concentration (Cmax) for all tissues but there is a significant difference between the profiles for 18 years old and 5 and 10 years old. There is reduced AUC and Cmax for 18 years old compared to 5 and 10 years old. Figure 4 shows observed data and simulated plasma concentration profiles (2.5th, 50th and 97.5th) following administration of 75 mg/m^2 intravenously and orally in children (mean age 13 years) with and without allopurinol [18]. The mean data is plotted with one SD bars at each time point. The mean data in these figures were used for parameters estimation. The predicted variability is satisfactory with possible over prediction for intravenous dosing. Figure 5 shows observed data and simulated plasma and RBC concentration profiles (2.5th, 50th and 97.5th) for children (mean age 9.6 years) following oral administration of 75 mg/m^2 [28]. The individual data points were digitized from the original publication and the mean profile was used in parameters estimation. The 95 % prediction interval shows slight under-prediction of both the plasma and RBC data but the trend is satisfactory. Figure 6 shows observed data and simulated plasma concentration profiles (2.5th, 50th and 97.5th) following administration of 50 mg/m^2/h 6-MP to children (mean age 10 years) as a 48 h infusion. The data is plotted as mean data and one SD bars at each time point. Both the mean data and the observed variability are predicted satisfactorily by the PBPK model. Figure 7 shows

Table 3 Other drug-specific parameters used in the PBPK model

Parameter	Definition	Value	Source
MW (g)	Molecular weight	152.2	–
fu	Plasma fraction unbound	0.81	[26, 27]
ka (h^{-1})	Absorption rate constant	0.28	–[a]
$CLG_{XO,ad}$ (L/h)	Intestinal clearance due to XO	25	–[b]
$CLL_{XO,ad}$ (L/h)	Hepatic clearance due to XO	36.5	–[b]
$CLPLAS_{ad}$ (L/h)	Plasma clearance	39.3	–[b]
PSBC (L/h)	RBC permeability-surface area product	145	–[b]
nP	RBC number of binding sites	0.079	–[b]
K_D (mg/L)	RBC dissociation constant	0.43	–[b]

[a] Fixed

[b] Estimated

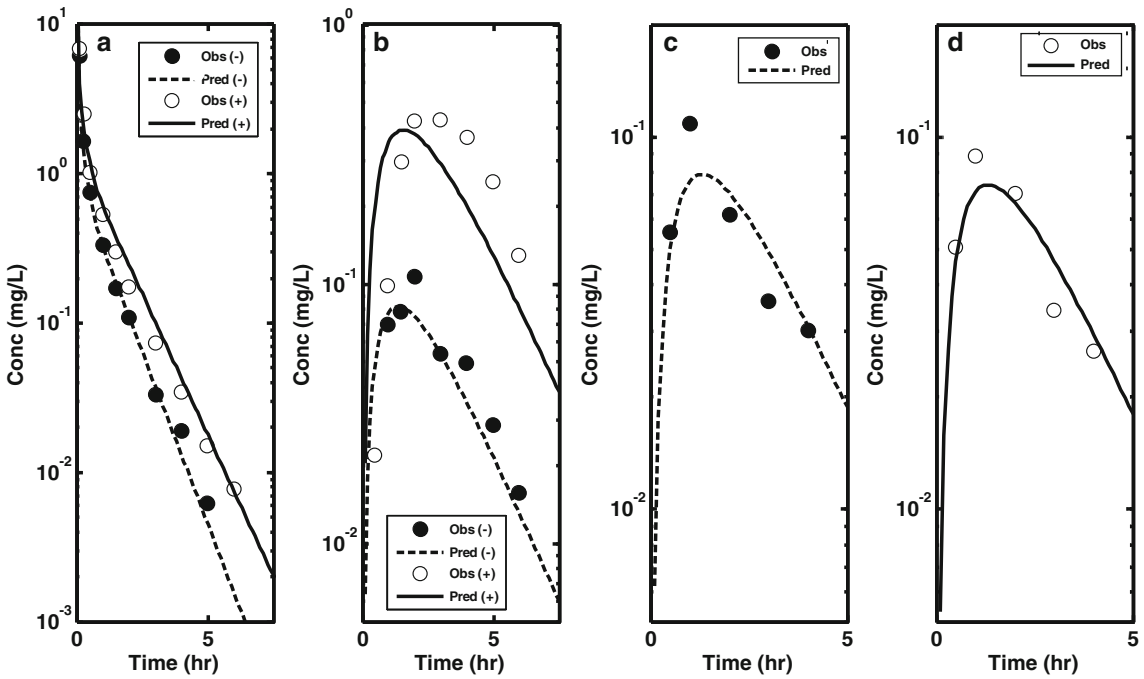

Fig. 2 Observed and predicted plasma and RBC concentration from the fitting. **a** Observed (Zimm et al. [18]) and predicted plasma concentration without (−) and with (+) allopurinol following IV dosing **b** Observed (Zimm et al. [18]) and predicted plasma concentration without (−) and with (+) allopurinol following oral dosing **c** Observed (Lafolie et al. [28]) and predicted plasma concentration following oral dosing **d** Observed (Lafolie et al. [28]) and predicted RBC concentration following oral dosing *Obs* observed data, *Pred* model prediction)

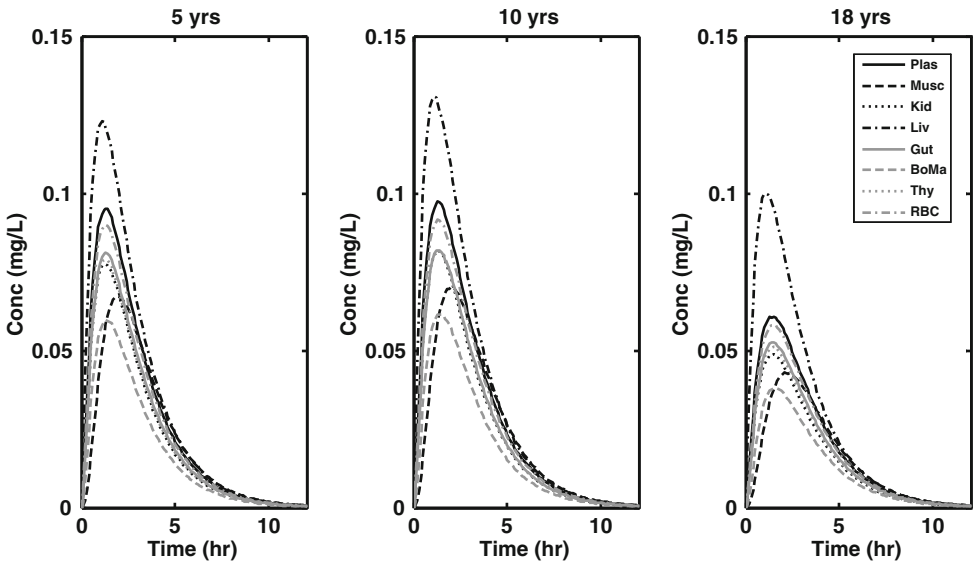

Fig. 3 Simulated mean concentration–time profiles of 6-mercaptopurine in plasma (Plas), muscle (Musc), kidney (Kid), liver (Liv), gut (Gut), bone marrow (BoMa), thymus (Thy) and red blood cells (RBC) following oral dosing of 75 mg/m^2 to 5, 10 and 18 years old subjects

observed data and simulated plasma and RBC concentration profiles (2.5th, 50th and 97.5th) for children from two studies. Figure 7a shows plasma data and simulated profiles following oral administration of 50 mg/m^2 to children (mean age 8.5 years) [3], Fig. 7b, c shows plasma and RBC data and simulated profiles respectively following oral administration of 75 mg/m^2 to children (mean age 9.8 years) [6]. The mean profiles and variabilities are satisfactorily predicted in all cases with possible slight overprediction of plasma data.

Figure 8 shows observed data and simulated plasma concentration profiles (2.5th, 50th and 97.5th) of 6-MP in children (mean age 7 years) following oral administration of 75 mg/m^2 alone (Fig. 8a) and combined with 20 mg/m^2

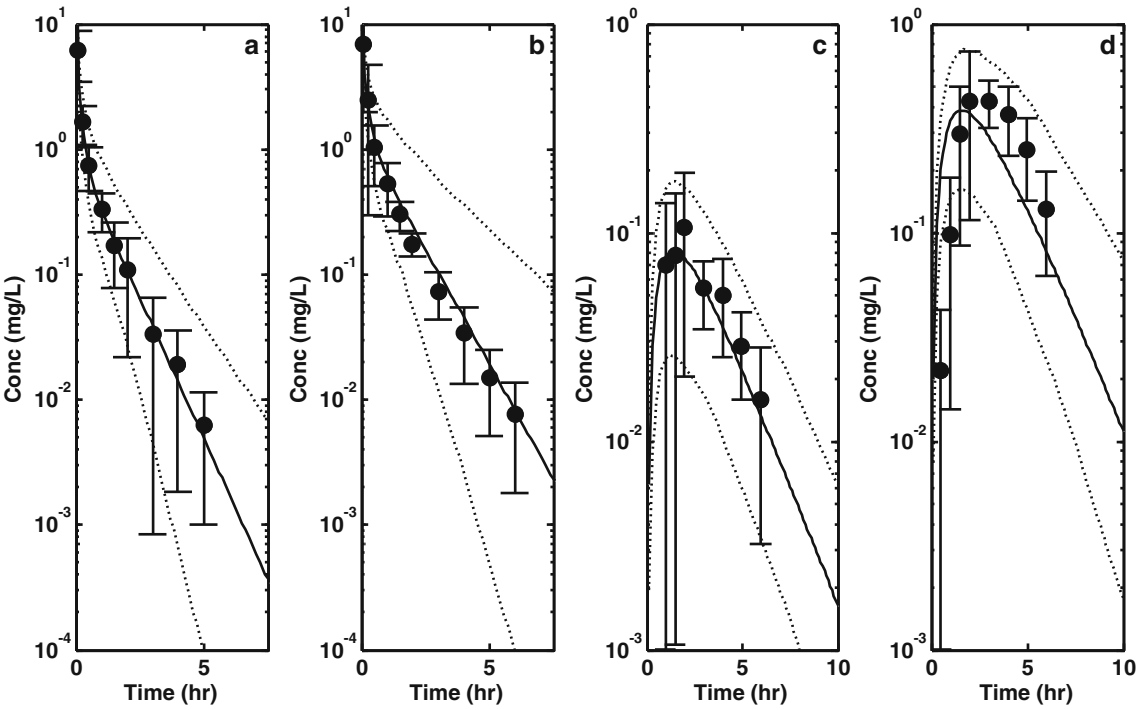

Fig. 4 Observed (Zimm et al. [18]) and simulated (2.5th, 50th and 97.5th) plasma concentration profile following administration of 75 mg/m^2 to children (mean age 13 years) intravenously and orally with and without allopurinol **a** IV without allopurinol **b** IV with allopurinol **c** PO without allopurinol **d** with allopurinol

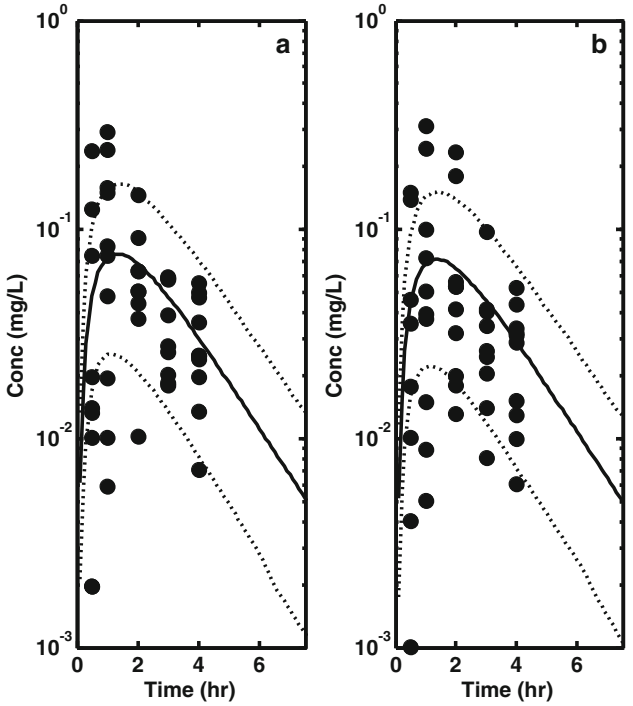

Fig. 5 Observed (Lafolie et al. [28]) and simulated (2.5th, 50th and 97.5th) **a** plasma and **b** RBC concentration profiles following oral administration of 75 mg/m^2 to children (mean age 9.6 years)

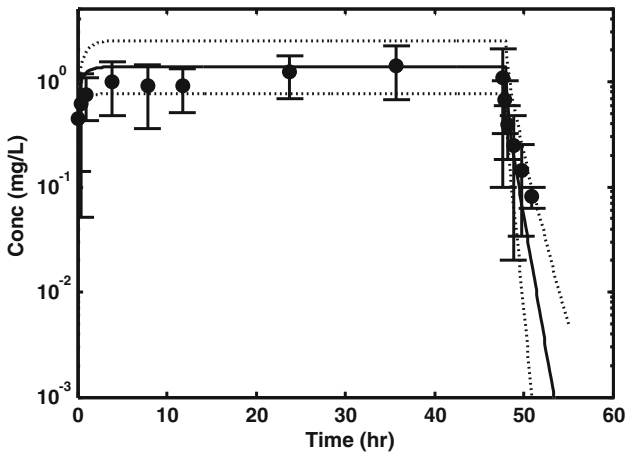

Fig. 6 Observed (Zimm et al. [37]) and simulated (2.5th, 50th and 97.5th) plasma concentration profiles following administration of 50 mg/m^2/h to children (mean age 10 years) as a 48 h infusion

of orally administered MTX (Fig. 8b) [14]. The data are plotted as mean data with one SD bars at each time points. The model slightly over predicts the observed 6-MP data (mean profile and variability) on both occasions. Also the difference between the mean profile of 6-MP on both occasions appears to be insignificant. The percentage dif-

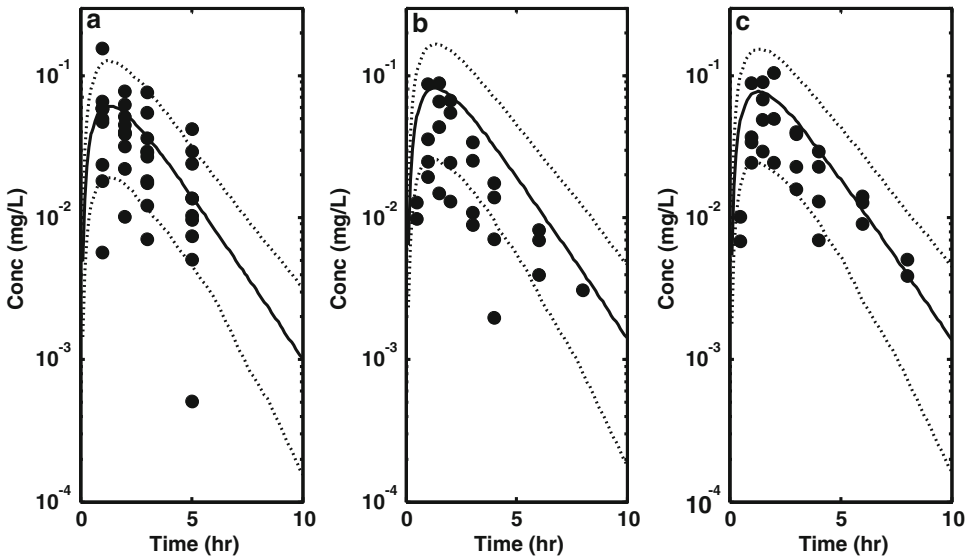

Fig. 7 Observed and simulated (2.5th, 50th and 97.5th) plasma and red blood concentration profiles **a** plasma following oral dosing of 50 mg/m^2 in children mean age 8.5 years (Mawatari et al. [3]) **b** plasma and **c** RBC following oral dosing of 75 mg/m^2 in children mean age 9.8 years (Lonnerholm et al. [6])

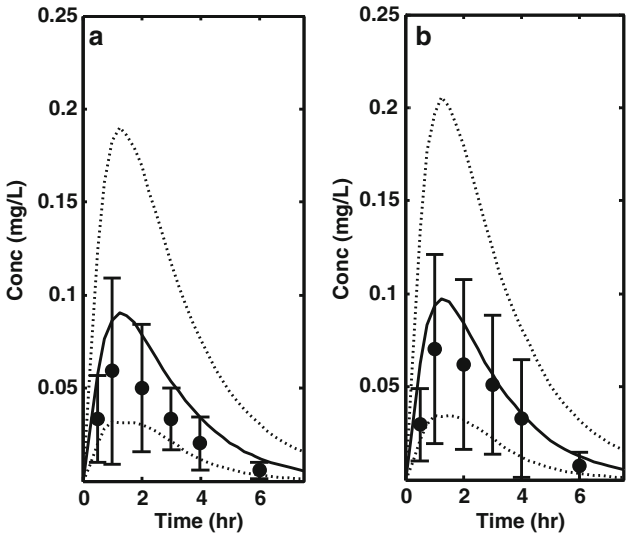

Fig. 8 Observed (Balis et al. [14]) and simulated (2.5th, 50th and 97.5th) plasma concentration profiles of 75 mg/m^2 oral 6-mercaptopurine in children, mean age 7 years (range 3–14 years) **a** 6-mercaptopurine only **b** 6-mercaptopurine co-administered with 20 mg/m^2 oral MTX

ference in AUC for predicted and observed are 5.5 and 31 % respectively and for Cmax are 7.3 and 26 % respectively. These results show under-prediction of the extent of interaction by the model. Figure 9 shows observed data and predicted plasma concentration profiles of MTX (Fig. 9a) and 6-MP (Fig. 9b) during maintenance treatment for four cycles in an ALL patient who was on stable 20 mg/m^2 orally administered MTX and 75 mg/m^2 orally administered 6-MP. The plots show adequate prediction of the MTX data and over-prediction of 6-MP data by the model. The plots also show that both observed and predicted variability in 6-MP is higher compared with MTX. Figure 10 shows simulated mean profiles of 6-MP following administration of 75 mg/m^2 orally administered 6-MP alone and co-administration of 75 mg/m^2 orally administered 6-MP and 5 g/m^2 of MTX administered as a 24 h infusion to 5, 10 and 18 years old. The profiles showed a significant change in AUC and Cmax with and without MTX. The percentage change in AUC and Cmax were 63.4 and 48.6 %, 62.7 and 47.0 % and 70.1 and 50.2 % for 5, 10 and 18 years old respectively. There is no significant difference between the mean profiles of 6-MP for 5 and 10 years old when the profiles are compared like-for-like, that is when profiles with and without MTX are compared separately. However profiles for 18 years old are reduced both in terms of AUC and Cmax when compared to the profiles for 5 and 10 years old when with and without profiles are compared separately.

Discussion and conclusion

This study has developed a PBPK model for plasma and tissue concentration prediction of 6-MP in adults and children following intravenous and oral dosing. The study is focused on childhood ALL patients as part of a project that is dedicated to the use of modelling and simulation in prediction of clinical trial outcomes in rare diseases. In childhood ALL, 6-MP is often used together with MTX in a number of protocols especially during maintenance treatment and therefore any potential interaction between the two drugs has to be accounted for adequately for efficient clinical trial simulation. In the first part of this work, a model was developed for MTX and in this part in addition to developing a model for 6-MP, the reported PK

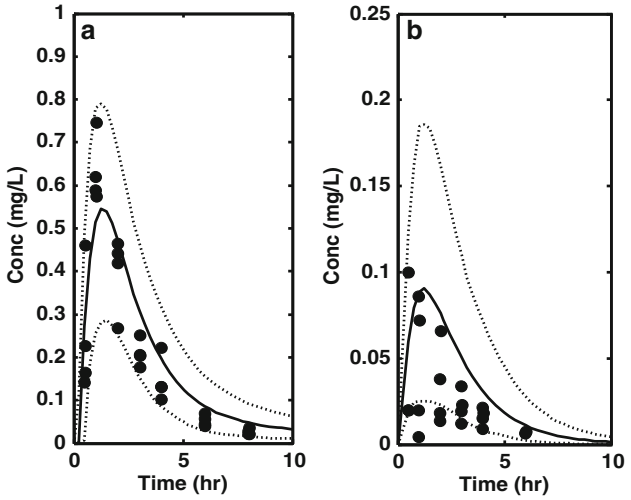

Fig. 9 Observed and predicted (2.5th, 50th and 97.5th profiles) plasma concentration of **a** Methotrate **b** 6-mercaptopurine obtained from four cycles of treatment from a single patient during maintenance treatment with stable 20 mg/m^2 of oral methotrexate and 75 mg/m^2 of oral 6-mercaptopurine

interaction between 6-MP and MTX was accounted for in the model.

The PBPK model developed for 6-MP in this work has separate compartments for key tissues/organs, these were linked through physiological blood flows and organ volumes. Since there was no clinical data available for model building in this project, published data was relied upon for both model building and validation. One advantage of using PBPK as opposed to conventional empirical compartmental modelling is that it is easier to combine data from different sources and age groups and also scaling beyond age groups that have been studied is more efficient through the use of age-dependent anatomical and physiological information available in the literature. In developing a PBPK model for 6-MP a method that has been described as in vitro-in vivo extrapolation [33] was combined with parameter estimation using observed clinical data. Information obtained from the literature from in vitro experiments was combined with physicochemical properties of the drug to predict the PK of 6-MP. Also, plasma and RBC concentration data were obtained from the literature to estimate other parameters that could not be predicted from in vitro experiments. Due to lack of data in adults in the literature, plasma and RBC concentration data for different paediatric age groups were used for parameter estimation, however the parameters (clearance) were scaled to adult. The data used to estimate the clearance parameters in the model were obtained from administration of 6-MP to children both by intravenous bolus and oral routes with and without allopurinol. The presence of data from the two routes allows estimation of clearance parameters responsible for first-pass effect of 6-MP through the presence of XO in the gut (CLG_{XO}) and the liver (CLL_{XO}) because allopurinol is a potent inhibitor of XO. Estimation of CLG_{XO} and CLL_{XO} was based on the assumption that allopurinol completely inhibits XO in the gut and the liver at the dose used in the clinical study. This assumption was partially tested by estimating a separate

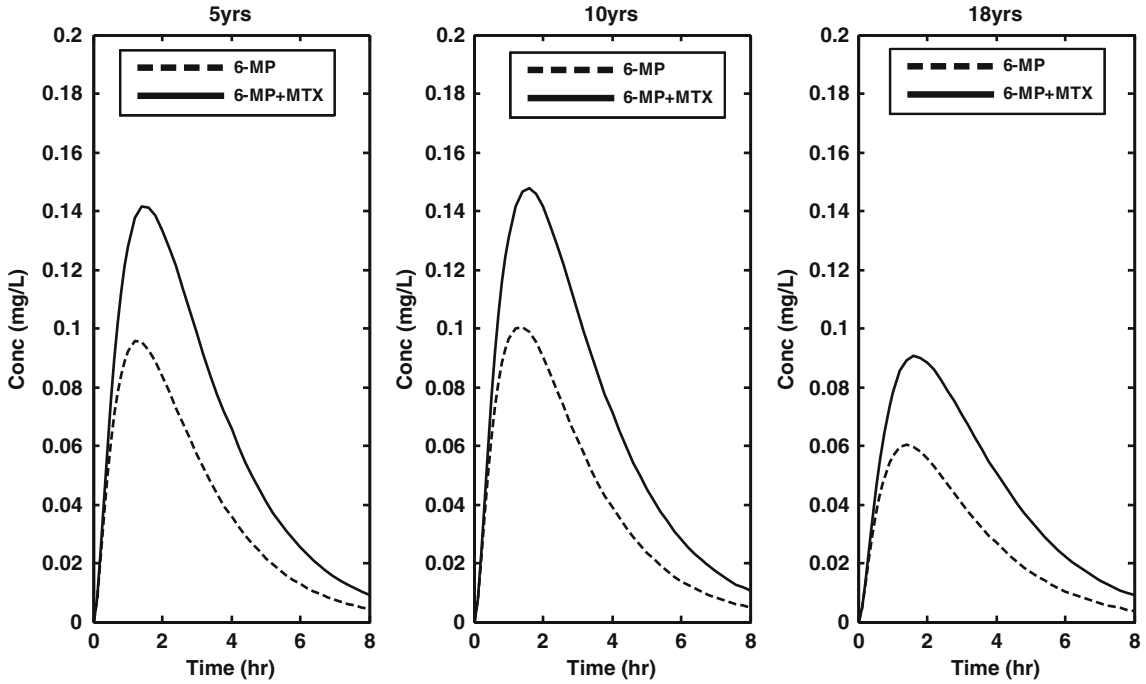

Fig. 10 Simulated mean profiles of oral 6-mercaptopurine (75 g/m^2) following co-administration with methotrexate (5 g/m^2) administered as a 24 h infusion to 5, 10 and 18 years old children

parameter due to XO in the gut and not inhibited by allopurinol. The parameter was identifiable from the available clinical data and the estimate obtained was 0.1 L/h. Since the estimate was insignificant the parameter was removed from the final analysis, this suggests that allopurinol as expected completely inhibit XO in the gut and the liver at the dose used in the clinical study.

K_ps are a very important component of PBPK models and a number of equations have been developed for their prediction when experimentally determined values in preclinical species are not available. This requires input parameters such as the physicochemical properties of the drug and fraction unbound in plasma. In this work the equation proposed by Poulin and Theil [24] has been used and the K_p for the rest of body was optimised so that predicted V_{SS} matches the observed value. The predicted V_{SS} using these K_ps was 0.66 L/kg and the reported values for V_{SS} in the literature for two different studies were 0.56 L/kg (SD = 0.38) [18] and 0.9 L/kg (SD = 0.3). The optimised K_p for the rest of body was 0.2 and the predicted K_p for adipose which made up of more than 50 % of the rest of body was 0.15. This shows that 6-MP distribution to adipose and other related tissues is limited.

Although 6-MP is metabolised by three competing routes, that is XO, HPRT and TPMT, only XO has been accounted for explicitly in the current work. Other routes have been accounted for by a plasma clearance parameter, mainly because there is no information on the activity of HPRT in all the tissues in which it has been reported to be present. HPRT has been reported to be widely distributed throughout the body, its activity has been demonstrated in tissues/organs such as erythrocyte, lymphocyte, liver, kidney, spleen and central nervous system. TPMT activity has been reported in tissues such as erythrocyte, lymphocytes, kidney and liver and the genetic polymorphism of this enzyme has also been widely discussed. Absence of TPMT activity in this model represents an important drawback of this work, its incorporation in the model will allow better prediction of tissue and plasma concentrations especially in different groups using genetic information. It is anticipated that it will be possible to incorporate TPMT activity in this model as more information becomes available in the literature on the role of 6-MP metabolites in the clinical effect of 6-MP and individual metabolite concentrations in the tissues are available. Individual plasma and metabolite concentrations in the tissues at different time points after dosing from different genetic polymorphic groups with different TPMT activity are necessary to further improve this model both in terms of development and validation. Information from in vitro experiments from the literature will be combined with parameter estimation to obtain estimates for other parameters in the model.

The PK interaction between 6-MP and MTX has also been predicted using the model developed for the two drugs incorporating inhibition of XO by MTX. There are limited clinical studies in the literature that have looked into the effect of MTX on the PK of 6-MP. The study by Balis et al. [14] reported modest clinical interaction between low oral dose MTX (20 mg/m^2) and a standard oral dose of 6-MP (75 mg/m^2) in children (31 and 26 % change in AUC and Cmax respectively). The model was able to predict an interaction between the two drugs although to a lower extent. Another study on the interaction between MTX and 6-MP in the literature is by Innocenti et al. [1]. A clinical interaction was reported in childhood ALL patients receiving daily oral doses of 6-MP (25 mg/m^2) and an intravenous infusion of high dose MTX (2 or 5 g/m^2 as 24 h infusion) once every other week. At 2 g/m^2 the reported change in AUC and Cmax were 69 and 108 % respectively and at 5 g/m^2 these were 93 and 121 % respectively. However there was an inconsistency in the results obtained in this study compared with other studies and that is why this interaction was not studied in the current work. The Cmax and AUC obtained by Innocenti et al. [1] when 25 mg/m^2 of 6-MP was given orally alone were comparable to what have been obtained in patients of similar age groups who are on three times the dose used in the study (75 mg/m^2 orally administered 6-MP) [14]. It is not clear why 25 mg/m^2 orally administered 6-MP was used in the study since the standard dose is 75 mg/m^2. However an attempt was made to investigate interaction between high dose MTX given as a 24 h intravenous infusion (5 g/m^2) and a standard oral dose of 6-MP (75 mg/m^2) in 5, 10 and 18 years old. The results showed significant changes in AUC and Cmax in the three age groups. The effect of MTX on the PK of 6-MP when MTX is given intravenously and 6-MP is given orally is through enterohepatic recirculation of MTX which has been accounted for in the model. When MTX is given intravenously, it is eliminated by the liver and via the gall bladder it is emptied into the gut lumen for reabsorption. During MTX reabsorption it inhibits XO in the enterocyte and hepatocytes thereby reducing the first-pass effect of XO on 6-MP bioavailability leading to increased AUC and Cmax.

The use of 6-MP in combination with MTX has shown remarkable improvement in cure of childhood ALL in the last 30 years. Despite the huge success, there is still considerable lack of effect and life threatening toxicity in some patients, possible due to substantial variability in the PK of 6-MP and its intracellular metabolites due to genetic polymorphism in the enzymes. Dose adjustment during treatment is still based on toxicity and therapeutic drug monitoring in not routinely used. The model developed in this work represents an attempt to improve dose individualisation and dosage regimen optimisation through modelling and simulation ultimately to achieve a better outcome in patients with childhood ALL. Although the focus of the work has been on childhood ALL, it can be

extended to other disease condition such as other types of cancer, Crohn's disease and ulcerative colitis.

In conclusion, a PBPK model has been developed for 6-MP, this model can be used to predict plasma and tissue concentrations in adults and children following intravenous and oral dosing. The model is focused on childhood ALL and PK interaction with MTX a drug commonly given in combination with 6-MP has been incorporated in the model. This model will help to improve clinical outcome in the use of 6-MP through better dosing.

Acknowledgments This work performed as part of Child-Rare-Euro-Simulation project. CRESim was funded by the ERA-NET PRIOMEDCHILD Joint Call in 2010. The authors also acknowledge helpful discussions with Dr. Aleksandra Galetin, Dr. Michael Gertz, Dr. Eleanor Howgate, Dr. Henry Pertinez, Mr. Nikolaos Tsamandouras, Mr. Adam Darwich and member of Centre for Applied Pharmacokinetic Research, Manchester Pharmacy School. Members of the CRESim Project Group: Leon Aarons; Agathe Bajard; Clément Ballot; Yves Bertrand; Frank Bretz; Daan Caudri; Charlotte Castellan; Sylvie Chabaud; Catherine Cornu; Frank Dufour; Nathalie Eymard; Roland Fisch; Renzo Guerrini; Vincent Jullien; Behrouz Kassaï; Patrice Nony; Kayode Ogungbenro; David Pérol; Gérard Pons; Harm Tiddens; Anna Rosati. Members of the Epi-CRESim Project Group: Corinne Alberti; Catherine Chiron; Catherine Cornu, Polina Kurbatova; Rima Nabbout.

Appendix 1

Equations that describe the concentration in each tissue/organ of the PBPK model for 6-mercaptopurine

(1) Systemic plasma

$$\begin{aligned} V_P\frac{dC_P}{dt} = {} & (Q_{HE}+Q_{GUT}+Q_{ENT}+Q_{SP})C_{LIV,V} \\ & + Q_{KID}C_{KID,V} + \frac{Q_{MU}C_{MU}}{K_{p,MU}} + \frac{Q_{SK}C_{SK}}{K_{p,SK}} + \frac{Q_{BM}C_{BM}}{K_{p,BM}} \\ & + \frac{Q_{TH}C_{TH}}{K_{p,TH}} + \frac{Q_{RE}C_{RE}}{K_{p,RE}} + Q_{HE} + Q_{GUT} + Q_{ENT} + Q_{KID} \\ & + Q_{MU} + Q_{SK} + Q_{SP} + Q_{BM} + Q_{TH} + Q_{RE})C_P \\ & - CLPLASC_P - PSBCfuC_P + PSBCC_{RBC,U} \end{aligned}$$

(2) Muscle

$$V_{MU}\frac{dC_{MU}}{dt} = Q_{MU}\left(C_P - \frac{C_{MU}}{K_{p,MU}}\right)$$

(3) Kidney

Vascular

$$\begin{aligned} V_{KID,V}\frac{dC_{KID,V}}{dt} = {} & Q_{KID}\left(C_P - C_{KID,V}\right) \\ & - CLPASS_{KID}fuC_{KID,V} \\ & + \frac{CLPASS_{KID}fuC_{KID,T}}{K_{p,KID}} \end{aligned}$$

Tissue

$$\begin{aligned} V_{KID,T}\frac{dC_{KID,T}}{dt} = {} & CLPASS_{KID}fuC_{KID,V} \\ & - \frac{CLPASS_{KID}fuC_{KID,T}}{K_{p,KID}} \end{aligned}$$

(4) Liver

Vascular

$$\begin{aligned} V_{LIV,V}\frac{dC_{LIV,V}}{dt} = {} & Q_{HE}\left(C_P - C_{LIV,V}\right) \\ & - CLPASS_{LIV}fuC_{LIV,V} + \frac{CLPASS_{LIV}fuC_{LIV,T}}{K_{p,LIV}} \\ & + \frac{(Q_{GUT}+Q_{ENT})C_{GUT}}{K_{p,GUT}} - (Q_{GUT}+Q_{ENT})C_{LIV,V} \\ & + \frac{Q_{SP}C_{SP}}{K_{p,SP}} - Q_{SP}C_{LIV,V} + Q_{ENT}C_{ENT} \end{aligned}$$

Tissue

$$\begin{aligned} V_{LIV,T}\frac{dC_{LIV,T}}{dt} = {} & CLPASS_{LIV}fuC_{LIV,V} - \frac{CLPASS_{LIV}fuC_{LIV,T}}{K_{p,LIV}} \\ & - \frac{CLL_{XO}fuC_{LIV,T}}{K_{p,LIV}} \end{aligned}$$

(5) Gut

Tissue

$$V_{GUT}\frac{dC_{GUT}}{dt} = (Q_{GUT}+Q_{ENT})\left(C_P - \frac{C_{GUT}}{K_{p,GUT}}\right)$$

Lumen

$$\frac{dA_{LUM}}{dt} = kgA_{ST} - kaA_{LUM} - ktA_{LUM}$$

Enterocyte

$$V_{ENT}\frac{dC_{ENT}}{dt} = kaA_{LUM} - Q_{ENT}C_{ENT} - CLG_{XO}C_{ENT}$$

(6) Stomach

$$\frac{dA_{ST}}{dt} = -kgA_{ST}$$

(7) Skin

$$V_{SK}\frac{dC_{SK}}{dt} = Q_{SK}\left(C_P - \frac{C_{SK}}{K_{p,SK}}\right)$$

(8) Bone Marrow

$$V_{BM}\frac{dC_{BM}}{dt} = Q_{BM}\left(C_P - \frac{C_{BM}}{K_{p,BM}}\right)$$

(9) Spleen

$$V_{SP}\frac{dC_{SP}}{dt} = Q_{SP}\left(C_P - \frac{C_{SP}}{K_{p,SP}}\right)$$

(10) Thymus

$$V_{TH}\frac{dC_{TH}}{dt} = Q_{TH}\left(C_P - \frac{C_{TH}}{K_{p,TH}}\right)$$

(11) Rest of the body

$$V_{RE}\frac{dC_{RE}}{dt} = Q_{RE}\left(C_P - \frac{C_{RE}}{K_{p,RE}}\right)$$

(12) Red blood cell

$$V_{RBC}\frac{dC_{RBC}}{dt} = PSBCfuC_P - PSBCC_{RBC,U}$$

$$C_{RBC,U} = \left(\sqrt{\left((nP + K_D - C_{RBC})^2 + (4K_DC_{RBC})\right)} - (K_D + nP - C_{RBC})\right)/2$$

6-MP and MTX interaction

Enterocyte

$$V_{ENT}\frac{dC_{ENT,6MP}}{dt} = ka_{6MP}A_{LUM,6MP} - Q_{ENT}C_{ENT,6MP} - \left(\frac{C_{ENT,6MP}CLG_{XO}}{1 + C_{ENT,MTX}/Ki}\right)$$

Liver tissue

$$V_{LIV,T}\frac{dC_{LIV,T(6MP)}}{dt} = CLPASS_{LIV}fu_{6MP}C_{LIV,V(6MP)} - \frac{CLPASS_{LIV}fu_{6MP}C_{LIV,T(6MP)}}{K_{p,LIV(6MP)}} - \frac{CLL_{XO}fu_{6MP}C_{LIV,T(6MP)}/K_{p,LIV(6MP)}}{1 + C_{LIV,T(MTX)}fu_{MTX}/Ki}$$

References

1. Innocenti F, Danesi R, Di Paolo A, Loru B, Favre C, Nardi M, Bocci G, Nardini D, Macchia P, Del Tacca M (1996) Clinical and experimental pharmacokinetic interaction between 6-mercaptopurine and methotrexate. Cancer Chemother Pharmacol 37: 409–414
2. Derijks LJ, Gilissen LP, Engels LG, Bos LP, Bus PJ, Lohman JJ, Curvers WL, Van Deventer SJ, Hommes DW, Hooymans PM (2004) Pharmacokinetics of 6-mercaptopurine in patients with inflammatory bowel disease: implications for therapy. Ther Drug Monit 26:311–318
3. Mawatari H, Unei K, Nishimura S, Sakura N, Ueda K (2001) Comparative pharmacokinetics of oral 6-mercaptopurine and intravenous 6-mercaptopurine riboside in children. Pediatr Int 43:673–677
4. Cheok MH, Evans WE (2006) Acute lymphoblastic leukaemia: a model for the pharmacogenomics of cancer therapy. Nat Rev Cancer 6:117–129
5. Zimm S, Collins JM, Riccardi R, O'Neill D, Narang PK, Chabner B, Poplack DG (1983) Variable bioavailability of oral mercaptopurine. Is maintenance chemotherapy in acute lymphoblastic leukemia being optimally delivered? N Engl J Med 308: 1005–1009
6. Lonnerholm G, Kreuger A, Lindstrom B, Ludvigsson J, Myrdal U (1986) Plasma and erythrocyte concentrations of mercaptopurine after oral administration in children. Pediatr Hematol Oncol 3:27–35
7. Lennard L (1992) The clinical pharmacology of 6-mercaptopurine. Eur J Clin Pharmacol 43:329–339
8. Balis FM, Holcenberg JS, Poplack DG, Ge J, Sather HN, Murphy RF, Ames MM, Waskerwitz MJ, Tubergen DG, Zimm S, Gilchrist GS, Bleyer WA (1998) Pharmacokinetics and pharmacodynamics of oral methotrexate and mercaptopurine in children with lower risk acute lymphoblastic leukemia: a joint children's cancer group and pediatric oncology branch study. Blood 92: 3569–3577
9. Matthews I, Kirkpatrick C, Holford N (2004) Quantitative justification for target concentration intervention—parameter variability and predictive performance using population pharmacokinetic models for aminoglycosides. Br J Clin Pharmacol 58:8–19
10. Tterlikkis L, Ortega E, Solomon R, Day JL (1977) Pharmacokinetics of mercaptopurine. J Pharm Sci 66:1454–1457
11. Hawwa AF, Collier PS, Millership JS, McCarthy A, Dempsey S, Cairns C, McElnay JC (2008) Population pharmacokinetic and pharmacogenetic analysis of 6-mercaptopurine in paediatric patients with acute lymphoblastic leukaemia. Br J Clin Pharmacol 66:826–837
12. Dervieux T, Hancock M, Evans W, Pui CH, Relling MV (2002) Effect of methotrexate polyglutamates on thioguanine nucleotide concentrations during continuation therapy of acute lymphoblastic leukemia with mercaptopurine. Leukemia 16:209–212
13. Giverhaug T, Loennechen T, Aarbakke J (1999) The interaction of 6-mercaptopurine (6-MP) and methotrexate (MTX). Gen Pharmacol 33:341–346
14. Balis FM, Holcenberg JS, Zimm S, Tubergen D, Collins JM, Murphy RF, Gilchrist GS, Hammond D, Poplack DG (1987) The effect of methotrexate on the bioavailability of oral 6-mercaptopurine. Clin Pharmacol Ther 41:384–387
15. Ogungbenro K, Matthews I, Looby M, Kaiser G, Graham G, Aarons L (2009) Population pharmacokinetics and optimal design of paediatric studies for famciclovir. Br J Clin Pharmacol 68: 546–560
16. Kawai R, Mathew D, Tanaka C, Rowland M (1998) Physiologically based pharmacokinetics of cyclosporine A: extension to tissue distribution kinetics in rats and scale-upto human. J Pharmacol Exp Ther 287:457–468
17. Kawai R, Lemaire M, Steimer JL, Bruelisauer A, Niederberger W, Rowland M (1994) Physiologically based pharmacokinetic study on a cyclosporin derivative, SDZ IMM 125. J Pharmacokinet Biopharm 22:327–365
18. Zimm S, Collins JM, O'Neill D, Chabner BA, Poplack DG (1983) Inhibition of first-pass metabolism in cancer chemotherapy: interaction of 6-mercaptopurine and allopurinol. Clin Pharmacol Ther 34:810–817
19. Johnson TN, Rostami-Hodjegan A, Tucker GT (2006) Prediction of the clearance of eleven drugs and associated variability in neonates, infants and children. Clin Pharmacokinet 45:931–956
20. Haycock GB, Schwartz GJ, Wisotsky DH (1978) Geometric method for measuring body surface area: a height-weight formula validated in infants, children, and adults. J Pediatr 93:62–66
21. DuBois D, DuBois EF (1916) A formula to estimate the approximate surface area if height and weight be known. Arch Intern Med 17:863–871
22. Valentin J (2002) Basic anatomical and physiological data for use in radiological protection: reference values: ICRP Publication 89. Ann ICRP 32:1–277
23. Yip R, Johnson C, Dallman PR (1984) Age-related changes in laboratory values used in the diagnosis of anemia and iron deficiency. Am J Clin Nutr 39:427–436
24. Poulin P, Theil FP (2000) A priori prediction of tissue:plasma partition coefficients of drugs to facilitate the use of

physiologically-based pharmacokinetic models in drug discovery. J Pharm Sci 89:16–35
25. Rodgers T, Rowland M (2007) Mechanistic approaches to volume of distribution predictions: understanding the processes. Pharm Res 24:918–933
26. Goodman LS, Gilman A (1996) Goodman & Gilman's the pharmacological basis of therapeutics/edited by Joel G. Hardman [et al.]. McGraw-Hill, Health Professions Division, New York, London
27. Loo TL, Luce JK, Sullivan MP, Frei E 3rd (1968) Clinical pharmacologic observations on 6-mercaptopurine and 6-methylthiopurine ribonucleoside. Clin Pharmacol Ther 9:180–194
28. Lafolie P, Hayder S, Bjork O, Ahstrom L, Liliemark J, Peterson C (1986) Large interindividual variations in the pharmacokinetics of oral 6-mercaptopurine in maintenance therapy of children with acute leukaemia and non-Hodgkin lymphoma. Acta Paediatr Scand 75:797–803
29. West GB, Brown JH, Enquist BJ (1999) The fourth dimension of life: fractal geometry and allometric scaling of organisms. Science 284:1677–1679
30. Lewis AS, Murphy L, McCalla C, Fleary M, Purcell S (1984) Inhibition of mammalian xanthine oxidase by folate compounds and amethopterin. J Biol Chem 259:12–15
31. GetData Graph Digitizer, http://getdata-graph-digitizer.com/. 2013
32. Beal S, Sheiner LB, Boeckmann A, Bauer RJ (2009) NONMEM User's Guides. (1989–2009). Icon Development Solutions, Ellicott City, MD, USA
33. Rostami-Hodjegan A, Tucker GT (2007) Simulation and prediction of in vivo drug metabolism in human populations from in vitro data. Nat Rev Drug Discov 6:140–148
34. Jamei M, Turner D, Yang J, Neuhoff S, Polak S, Rostami-Hodjegan A, Tucker G (2009) Population-based mechanistic prediction of oral drug absorption. The AAPS Journal 11:225–237
35. Gertz M, Houston JB, Galetin A (2011) Physiologically based pharmacokinetic modeling of intestinal first-pass metabolism of CYP3A substrates with high intestinal extraction. Drug Metab Dispos 39:1633–1642
36. Symcyp. Simcyp Limited, Sheffield, UK. 2008
37. Zimm S, Ettinger LJ, Holcenberg JS, Kamen BA, Vietti TJ, Belasco J, Cogliano-Shutta N, Balis F, Lavi LE, Collins JM et al (1985) Phase I and clinical pharmacological study of mercaptopurine administered as a prolonged intravenous infusion. Cancer Res 45:1869–1873